

1 **Effect of sporadic destratification, seasonal overturn and**
2 **artificial mixing on CH₄ emissions at the surface of a**
3 **subtropical hydroelectric reservoir (Nam Theun 2**
4 **Reservoir, Lao PDR)**

5 **F. Guérin^{1,2,3,*}, C. Deshmukh^{1,4,5,a}, D. Labat¹, S. Pighini^{6,b}, A Vongkhamsao⁶, P.**
6 **Guédant⁶, W. Rode⁶, A. Godon^{6,c}, V. Chanudet⁷, S. Descloux⁷, D. Serça⁴**

7 [1]{Université de Toulouse ; UPS GET, 14 Avenue E. Belin, F-31400 Toulouse, France}

8 [2]{IRD ; UR 234, GET ; 14 Avenue E. Belin, F-31400, Toulouse, France}

9 [3]{Departamento de Geoquímica, Universidade Federal Fluminense, Niteroi-RJ, Brasil}

10 [4]{Laboratoire d'Aérodologie - Université de Toulouse - CNRS UMR 5560; 14 Av. Edouard
11 Belin, F-31400, Toulouse, France}

12 [5]{Centre for Regulatory and Policy Research, TERI University, New Delhi, India}

13 [6]{Nam Theun 2 Power Company Limited (NTPC), Environment & Social Division – Water
14 Quality and Biodiversity Dept.– Gnommalath Office, PO Box 5862, Vientiane, Lao PDR}

15 [7]{Electricité de France, Hydro Engineering Centre, Sustainable Development Dpt, Savoie
16 Technolac, F-73373 Le Bourget du Lac, France}

17 [a]{now at: Nam Theun 2 Power Company Limited (NTPC), Environment & Social Division
18 – Water Quality and Biodiversity Dept.– Gnommalath Office, PO Box 5862, Vientiane, Lao
19 PDR}

20 [b]{now at: Innsbruck University, Institute of Ecology, 15 Sternwartestrasse, A-6020
21 Innsbruck, Austria and Foundation Edmund Mach, FOXLAB-FEM, Via E. Mach 1, IT-38010
22 San Michele all'Adige, Italy}

23 [c]{now at: Arnaud Godon Company, 44 Route de Genas, Nomade Lyon, 69003 Lyon,
24 France}

25
26 *Correspondence to: F Guérin (Frederic.guerin@ird.fr)

27 **Abstract**

28 Inland waters in general and specifically freshwater reservoirs are recognized as source of
29 CH₄ to the atmosphere. Although the diffusion at the air-water interface is the most studied
30 pathway, its spatial and temporal variations are poorly documented.

31 We measured fortnightly CH₄ concentrations and physico-chemical parameters at nine
32 stations in a subtropical monomictic reservoir which was flooded in 2008 (Nam Theun 2
33 Reservoir, Lao PDR). Based on these results, we quantified CH₄ storage in the water column
34 and diffusive fluxes from June 2009 to December 2012. We compared diffusive emissions
35 with ebullition from Deshmukh et al. (2014) and aerobic methane oxidation and downstream
36 emissions from Deshmukh et al. (2015).

37 In this monomictic reservoir, the seasonal variations of CH₄ concentration and storage were
38 highly dependant of the thermal stratification. Hypolimnic CH₄ concentration and CH₄
39 storage reached their maximum in the warm dry season (WD) when the reservoir was
40 stratified. They decreased during the warm wet (WW) season and reached its minimum after
41 the reservoir overturned in the cool dry season (CD). The sharp decreases of the CH₄ storage
42 were concomitant with sporadic extreme diffusive fluxes (up to 200 mmol m⁻² d⁻¹). These hot
43 moments of emissions occurred mostly in the inflow region in the WW season and during the
44 overturn in the CD season in the area of the reservoir that has the highest CH₄ storage.
45 Although they corresponded to less than 10% of the observations, these CH₄ extreme
46 emissions (>5 mmol m⁻² d⁻¹) contributed up to 50% of total annual emissions by diffusion.

47 During the transition between the WD and WW seasons, a new hotspot of emissions was
48 identified upstream of the water intake where diffusive fluxes peaked at 600 mmol m⁻² d⁻¹ in
49 2010 down to 200 mmol m⁻² d⁻¹ in 2012. In the CD season, diffusive fluxes from this area
50 were the lowest observed at the reservoir surface. Emissions from this area contributed 15-
51 25% to total annual emissions although they occur on a surface area representative of less
52 than 1% of the total reservoir surface. We highly recommend measurements of diffusive
53 fluxes around water intakes in order to evaluate if such results can be generalized.

54 **1. Introduction**

55 Since the 1990s, hydroelectric reservoirs are known to be source of methane (CH₄) to the
56 atmosphere. Their contribution to total CH₄ emissions still needs refinement since the
57 discrepancies among estimates is large, ranging from 1 to 12% of total CH₄ emissions (St
58 Louis et al., 2000;Barros et al., 2011). These two estimates are mostly based on diffusive

59 fluxes at the air-water interface and they overlook emissions from the rivers downstream of
60 the dams (Abril et al., 2005;Guerin et al., 2006;Kemenes et al., 2007;Teodoru et al.,
61 2012;Maeck et al., 2013;Deshmukh et al., 2015), CH₄ ebullition (DelSontro et al.,
62 2010;Deshmukh et al., 2014) and emissions from the drawdown area of reservoirs (Chen et
63 al., 2009;Chen et al., 2011) although these pathways could largely dominate diffusion at the
64 surface of the reservoirs.

65 Even if CH₄ diffusion at the surface of reservoir is the best-documented emission pathway,
66 little information is available on spatial and temporal variability of CH₄ emissions by
67 diffusive fluxes. In tropical amictic reservoirs, the highest diffusive fluxes are usually
68 observed during dry periods and when the stratification weaken at the beginning of the rainy
69 season (Guerin and Abril, 2007). A study of CH₄ emissions from a dimictic reservoir suggests
70 a potential large outgassing of CH₄ during the reservoir overturns (Utsumi et al., 1998b) as it
71 is the case in natural monomictic and dimictic lakes (Kankaala et al., 2007;López Bellido et
72 al., 2009;Schubert et al., 2010;Schubert et al., 2012;Fernández et al., 2014). Such hot
73 moments of emissions (McClain et al., 2003) could contribute 45-80% of CH₄ annual
74 emissions by diffusion (Schubert et al., 2012;Fernández et al., 2014). They are rarely taken
75 into account in carbon budgets since they can only be captured by high frequency monitoring.
76 Spatial heterogeneity of CH₄ emissions at the surface of reservoirs is also very high. It mostly
77 depends on the spatial variations of ebullition that is controlled by sedimentation (DelSontro
78 et al., 2011;Sobek et al., 2012;Maeck et al., 2013). The spatial variation of diffusion appears
79 to be low with emissions being slightly higher (1) in area where dense forest is flooded as
80 compare to the former riverbed (Abril et al., 2005), (2) at shallow sites than at deeper ones
81 (Zheng et al., 2011;Sturm et al., 2014) and (3) in inflow zones of reservoirs compare to the
82 main body (Musenze et al., 2014). However, as it was shown for CO₂ emissions from a
83 tropical hydroelectric reservoir, taking into account both spatial and temporal variability of
84 emissions significantly affect carbon budgets and emission factors (Pacheco et al., 2015).

85 The spatial and temporal variability of CH₄ ebullitive fluxes were intensively studied at the
86 newly flooded subtropical Nam Theun 2 Reservoir (NT2R) (Deshmukh et al., 2014) and
87 downstream as well as total CH₄ emissions are described in Deshmukh et al. (2015). The
88 objective of the present study is to quantify the CH₄ diffusive fluxes at the surface of NT2R.
89 The CH₄ emissions were quantified fortnightly during three and a half year (May 2010 to
90 December 2012) based on a monitoring of CH₄ concentrations that started in June 2009. This
91 was performed at nine stations flooding different types of ecosystems. On the basis of these

92 results, we discuss the spatial and temporal variations of the CH₄ emissions by diffusive
93 fluxes and the significance of hotspots and hot moments in the total emissions from the
94 surface of the reservoir.

95 **2. Material and methods**

96 **2.1. Study area**

97 The NT2 hydroelectric reservoir (17° 59' 49" N, 104° 57' 08" E) was built on the Nam Theun
98 River located in the subtropical region of Lao People's Democratic Republic (Lao PDR) on
99 the Nakai Plateau. A detailed description of the study site is given in Descloux et al. (2014).
100 The filling of the reservoir began in April 2008, the full water level was first reached in
101 October 2009 and the power plant was commissioned in April 2010. Annually, the NT2
102 Reservoir receives around 7527 Mm³ of water from the Nam Theun watershed, which is more
103 than twice the volume of the reservoir (3908 Mm³). A continuous flow of 2 m³ s⁻¹ (and
104 occasionally spillway release) is discharged from the Nakai Dam (ND in Fig 1) to the Nam
105 Theun River. The water used for electricity production is delivered from water intake (WI in
106 Fig 1) to the powerhouse (PH in Fig 1). The powerhouse is located in the valley 200 m below
107 the plateau.

108 Typical meteorological years are characterized by three seasons: warm wet (WW) (mid June-
109 mid October), cool dry (CD) (mid October-mid February) and warm dry (WD) (mid
110 February-mid June). Daily air temperature varies between 14°C (CD season) to 30°C (WD
111 season). The mean annual rainfall is about 2400 mm and occurs mainly (80%) in the WW
112 season.

113 During the filling of the reservoir, 489 km² of soils and different types of vegetation
114 (Descloux et al., 2011) were flooded by the end of October 2008. The water level in the
115 reservoir was nearly constant from October 2008 to April 2010. After the commissioning,
116 during the studied period (June 2009 to December 2012) the reservoir surface varied
117 seasonally and reached its maxima (489 km²) and minima (168 to 176 km² depending on the
118 years) during the WW and WD seasons, respectively. According to these water level
119 variations, the average depth is 8 m for a maximum depth of 39 m.

120 **2.2. Sampling strategy**

121 A total of nine stations (RES1-9, Figure 1) located in the reservoir were monitored fortnightly
122 in order to determine the vertical profiles of physico-chemical parameters of the water column
123 and the CH₄ concentrations. The characteristics of the stations are given in the Table 1.
124 Basically, three stations are located on the thalweg of the former Nam Theun River (RES2,
125 RES4, RES6) whereas four other stations are located in a small embayment in the flooded
126 dense forest (RES3), flooded degraded forest (RES5), flooded swamp area (RES7) and
127 flooded agricultural land (RES8). The RES1 station is located 100 m upstream of the Nakai
128 Dam, and RES9 station is located ~1 km upstream of the water intake delivering the water to
129 the powerhouse. All samples and in situ measurements were taken in the morning or early
130 afternoon from an anchored boat. Most of the time, the boat was attached to a buoy at the
131 sampling station. When no buoy was present, an anchor was used with care in order not to re-
132 suspend surface sediments. As the sampling started from the surface, the bottom water was
133 sampled almost an hour later and should not be influenced by the perturbation generated by
134 the anchor.

135 **2.3. Experimental methods**

136 **2.3.1. Vertical profiles of oxygen and temperature**

137 Vertical profiles of O₂ and temperature were measured in situ at all sampling stations with a
138 multi-parameter probe Quanta[®] (Hydrolab, Austin, Texas) since January 2009. In the
139 reservoir, the vertical resolution was 0.5 m above the oxic–anoxic limit and 1 to 5 m in the
140 hypolimnion.

141 **2.3.2. Methane concentration in water**

142 The evolution of CH₄ concentrations has been monitored from May 2009 to December 2012
143 on a fortnightly basis. Surface samples were taken with a surface water sampler (Abril et al.,
144 2007) and other samples from the water column were taken with an Uwitec water sampler.
145 (Abril et al., 2007). Water samples were stored in serum glass vials, capped with butyl
146 stoppers, sealed with aluminium crimps and poisoned (Guerin and Abril, 2007). Before gas
147 chromatography analysis for CH₄ concentration, a N₂ headspace was created and the vials
148 were vigorously shaken to ensure an equilibration between the liquid and gas phases. The

149 concentration in the water was calculated using the solubility coefficient of Yamamoto et al.
150 (1976).

151 **2.3.3. Gas chromatography**

152 Analysis of CH₄ concentrations were performed by gas chromatography (SRI 8610C gas
153 chromatograph, Torrance, CA, USA) equipped with a flame ionization detector. A subsample
154 of 0.5 ml from the headspace of water sample vials was injected. Commercial gas standards
155 (10, 100 and 1010 ppmv, Air Liquid "crystal" standards) were injected after analysis of every
156 10 samples for calibration. Duplicate injection of samples showed reproducibility better than
157 5%.

158 **2.4. Water column CH₄ storage**

159 Between two sampling depth of the vertical profiles of CH₄ concentrations, the CH₄
160 concentrations were assumed to change linearly in order to calculate the concentration in each
161 1-m layer of water. The volume of water in each layer was calculated using the volume-
162 capacity curve (NTPC, 2005). The CH₄ storage was calculated by multiplying the average
163 CH₄ concentrations of each layer by the volume of the layer and summing-up the amount of
164 CH₄ for all depth intervals.

165 **2.5. Aerobic CH₄ oxidation**

166 The depth-integrated CH₄ oxidation rates at each station were calculated on the basis of the
167 specific oxidation rates (d⁻¹) determined at NT2 (Deshmukh et al., 2015) and the vertical
168 profiles of CH₄ and O₂ concentrations in the water column as already described in (Guerin
169 and Abril, 2007). The depth-integrated CH₄ oxidation rates at each station were estimated
170 only from January 2010 since the vertical resolution of the vertical profiles of O₂ and CH₄
171 was not high enough in 2009.

172 **2.6. Estimation of diffusive fluxes from surface concentrations**

173 The diffusive CH₄ fluxes were calculated from the fortnightly monitoring of surface
174 concentrations with the thin boundary layer (TBL) equation at all stations in the reservoir
175 (RES1-9). The CH₄ surface concentrations in water and the average CH₄ concentration in air
176 (1.9 ppmv) obtained during eddy covariance deployments (Deshmukh et al., 2014) were
177 applied in equation (1) to calculate diffusive flux:

178
$$F = k_T \times \Delta C \tag{1}$$

179 where F , the diffusive flux at water-air interface; k_T , the gas transfer velocity at a given
180 temperature (T); $\Delta C = C_w - C_a$, the concentration gradient between the water (C_w) and the
181 concentration at equilibrium with the overlying atmosphere (C_a). Afterward, the k_T was
182 computed from k_{600} with the following equation:

183
$$k_T = k_{600} \times (600/Sc_T)^n \tag{2}$$

184 with Sc_T , the Schmidt number of CH_4 at a given temperature (T) (Wanninkhof, 1992); n , a
185 number that is either $2/3$ for low wind speed ($< 3.7 \text{ m s}^{-1}$) or $1/2$ for higher wind speed and
186 turbulent water (Jahne et al., 1987).

187 For the determination of k_{600} at the stations RES1-8, we used both the formulations from
188 Guerin et al. (2007) which includes the cumulative effect of wind (U_{10}) and rain (R) on k_{600}
189 ($k_{600} = 1:66e^{0:26U_{10}} + 0:66R$), and the average formulation of MacIntyre et al. (2010) ($k_{600} =$
190 $2.25 U_{10} + 0.16$) whatever the buoyancy fluxes. As shown by (Deshmukh et al., 2014), the
191 average of the fluxes obtained from these two relationships compared well with fluxes
192 measured by floating chambers at the reservoir surface and no enhancement of the CH_4 fluxes
193 could have been attributed to the variations of buoyancy fluxes when the eddy covariance
194 system was deployed. Since the water current velocities were lower than 1 cm s^{-1} in most of
195 the reservoir (Chanudet et al., 2012), the effect of water current on k_{600} was not included. For
196 calculation purpose, wind speed (at 10 m height) and rainfall from two adjacent
197 meteorological stations located at Nakai Village (close to RES9 station) and at the Ban
198 Thalang Bridge (close to RES4 station, Figure 1) were used. At these stations, the average
199 k_{600} was 6.5 cm h^{-1} over the course of the year.

200 At the water intake (RES9) where the hydrology and hydrodynamics is different from the
201 other stations, it was impossible to quantify the k_{600} since the boat drifted quickly to the
202 shoreline because of water currents in the narrow channel. According to Chanudet et al.
203 (2012), water current velocity in this area of the reservoir is about 0.2 m s^{-1} . After Borges et
204 al. (2004), the contribution of such water currents in a water body with depth ranging from 9
205 to 20 m is $2.0 \pm 0.5 \text{ cm h}^{-1}$ which should be summed up with the contribution of wind and
206 rainfall from Guerin et al. (2007) and MacIntyre et al. (2010). It gives an average of 9 cm h^{-1} .
207 The k_{600} was determined in the regulating dam (Deshmukh et al., 2014) located downstream
208 of the turbine where we visually observed vortexes similar to those observed at RES9. In the

209 regulating dam, the k_{600} was 19 cm h^{-1} on average for 4 measurements (not show). In order to
210 be conservative for the estimation of emissions from the water intake, we considered a
211 constant value of k_{600} (10 cm h^{-1}) which is in the lower range of (1) the k_{600} calculated from
212 (Guerin et al., 2007), MacIntyre et al. (2010) and Borges et al. (2004), and (2) k_{600} values
213 determined in area with comparable hydrology/hydrodynamics.

214 **2.7. Extrapolation of fluxes for the estimation of the NT2 total emissions**

215 Based on physical modelling (Chanudet et al., 2012), it has been showed that the station
216 RES9 located at the water intake is representative of an area of $\sim 3 \text{ km}^2$ (i.e. 0.6% of reservoir
217 water surface), whatever the season. This 3- km^2 area was used to extrapolate specific
218 diffusive fluxes from RES9. The embayment where RES3 is located represents a surface area
219 of 5-6% of the total surface area of the reservoir whatever the season (maximum 28 km^2), to
220 which were attributed the specific diffusive fluxes from RES3. The diffusive fluxes calculated
221 for RES1, RES2, RES4, RES5, RES6, RES7 and RES8 stations were attributed to the water
222 surface area representative for each station, taking into account the seasonal variation of the
223 reservoir water surface from the surface-capacity curve (NTPC, 2005).

224 **2.8. Statistical and correlation analysis**

225 Statistical tests were performed to assess the spatial and temporal variations in the surface
226 CH_4 concentrations and diffusive fluxes at all stations in the reservoir. Normality of the
227 concentration and diffusive datasets was tested with R software (R Development Core Team,
228 2008) and the Nortest package (Gross and Ligges, 2015). The data distribution was tested
229 with the Fitdistrplus package (Delignette-Muller et al., 2015).

230 Since all tests indicated that the distribution of the data were neither normal nor lognormal,
231 Kruskal-Wallis and Mann-Whitney tests were performed with GraphPad Prism (GraphPad
232 Software, Inc., v5.04). No significant differences were found between the seasons and/or the
233 stations. These test results were attributed to the very large range of surface concentrations
234 due to the sporadic occurrence of extreme values (over 4 orders of magnitude). In order to
235 reduce this range, the log of the concentrations was used. For each station, the time series of
236 the log of the CH_4 surface concentrations were linearly interpolated and re-sampled every 15
237 days in order to compare time series with the same number of observations. The log of the
238 concentrations was used to determine the frequency distribution, the skewness of the dataset

239 (third order moment), the auto-correlation of each time series and the correlation between the
240 different stations. All analyses were performed using Matlab.

241 **3. Results**

242 **3.1. Temperature and O₂ dynamics in the reservoir water column**

243 During the three and half year of monitoring at the stations RES1-8, the NT2R was thermally
244 stratified with a thermocline at 4.5 ± 2.6 m depth in the WD (Feb-Jun) season as revealed by
245 the vertical profiles of temperature (Figure 2). In the WW season, the temperature vertical
246 profiles at the stations RES1-8 either showed a thermocline (RES7 and RES8 in 2010 and
247 2011, Figure 2) whereas in some occasions, the temperature decreased regularly from the
248 surface to the bottom during sporadic destratification (RES1-3, Figure 2). On average during
249 the WW season, a thermocline was located at 5.8 ± 4.8 m depth. During the CD season, the
250 reservoir overturned as already mentioned by Chanudet et al. (2012) and the temperature was
251 constant from the surface to the bottom (Figure 2) in the different years. In order to illustrate
252 the destratification, a stratification index (ΔT) which corresponds to the difference between
253 the surface and bottom water temperature was defined. During the periods of stratification in
254 the WD seasons, ΔT was up to 10°C higher than during reservoir overturn in the CD season
255 with ΔT close to zero (Figure 3a). During the WW season, the ΔT decreased gradually.

256 During the WD season at the stations RES1-8, an oxicleine was most of the time located at a
257 depth concomitant with the depth of the thermocline whereas oxygen penetrated deeper in the
258 WW season (Figure 2). During these two seasons, the epilimnion was always well oxygenated
259 with O₂ concentrations higher than $200 \mu\text{mol L}^{-1}$. In the WD season, the hypolimnion was
260 completely anoxic whereas O₂ reached occasionally the hypolimnion during the sporadic
261 destratification events in the WW season ($29 \pm 54 \mu\text{mol L}^{-1}$, Figure 2 and 3b). During the CD
262 season (reservoir overturn), the water column was often oxygenated from the top to the
263 bottom of the reservoir (Figure 2). On average over the whole reservoir, the lowest
264 hypolimnic oxygen concentration was observed in 2010 before the reservoir was
265 commissioned (Figure 3b).

266 After the commissioning of the reservoir (April 2010), the water column located near the
267 water intake (RES9) got totally mixed as revealed by the homogeneous temperature and
268 oxygen profiles from the surface to the bottom whatever the season (Figure 2). The water
269 column at RES9 was always well oxygenated ($163 \pm 62 \mu\text{mol L}^{-1}$, Figure 2).

270 **3.2. Seasonal dynamics of the CH₄ concentration and storage in the reservoir water**
271 **column**

272 At the station RES1-8, when the water column is thermally stratified with a steep oxicleine in
273 the WD and often in the WW seasons, CH₄ concentrations are in average ~150 times higher in
274 the reservoir hypolimnion ($246 \pm 234 \mu\text{mol L}^{-1}$) than in the epilimnion ($1.6 \pm 7.7 \mu\text{mol L}^{-1}$)
275 (Figure 2). The gradient of CH₄ concentration at the thermocline/oxicleine was steeper during
276 the WD season than during the WW season (Figure 2). During the CD season, the average
277 CH₄ concentration in the reservoir bottom water lowered by a factor of three compare to the
278 WD and the WW seasons. However, the reservoir overturn increased the average CH₄
279 concentrations in the epilimnion by a factor of two ($3.4 \pm 14.8 \mu\text{mol L}^{-1}$) in comparison with
280 the WD and WW seasons. After the commissioning, the CH₄ vertical profiles of concentration
281 before turbine intake (RES9) were homogeneous from the surface to the bottom. The average
282 CH₄ concentration from the surface to the bottom peaked up to $215 \mu\text{mol L}^{-1}$ with averages of
283 39.8 ± 48.8 , 29.9 ± 55.4 and $1.9 \pm 4.3 \mu\text{mol L}^{-1}$ during the WD, WW and CD seasons,
284 respectively (Figure 2). The concentrations at RES9 were up to 10 times lower than the
285 maximum bottom concentrations at the other stations for a given season. Since the station
286 RES9 behaved differently from the other stations, results from this station will be treated
287 separately.

288 The overall bottom CH₄ concentration (Figure 3c) and dissolved CH₄ stock in the reservoir
289 (Figure 3d) increased at the beginning of the WD season. The higher bottom CH₄
290 concentration and storage in the reservoir are concomitant with both the establishment of
291 anoxia in the hypolimnion and the reservoir thermal stratification (Figure 3). Hypolimnic CH₄
292 concentration and storage reached their maxima (up to $508 \pm 254 \mu\text{mol L}^{-1}$ and 4.7 ± 0.5
293 $\text{Gg}(\text{CH}_4)$, Figure 3c,d) at the end of the WD-beginning of the WW season when the residence
294 time of water in the reservoir was the lowest (40 days, Figure 3d). Along the WW season, the
295 thermal stratification weakened (Figure 3a) and the CH₄ concentration and dissolved CH₄
296 stock decreased (Figure 3c,d) while the residence time of water increased (Figure 3d). In the
297 CD season, the reservoir overturns as evidenced by the low ΔT and the penetration of O₂ to
298 the hypolimnion (Figure 3a,b). During CD season, the bottom CH₄ concentration and the
299 storage reached their minima (down to $1.3 \pm 4.5 \mu\text{mol L}^{-1}$ and $0.01 \pm 0.001 \text{Gg}(\text{CH}_4)$, Figure
300 3c,d) when the residence time of water was the longest (Figure 3d). The sharp decrease of
301 CH₄ storage and concentration in the transition from the WW to the CD seasons is

302 concomitant with a sharp increase of O₂ concentration at the bottom (up to 160 ± 89 μmol L⁻¹,
303 Figure 3).

304 **3.3. Interannual variations of the CH₄ concentrations and storage in the reservoir** 305 **water column**

306 During the three and a half years of monitoring, the same seasonal pattern is observed
307 although the annual CH₄ bottom concentration and storage was threefold higher in 2009 and
308 2010 than in the year 2011 (Figure 3c,d). In the dry year 2012, the reservoir bottom CH₄
309 concentration and storage was almost twice higher than in wet year 2011.

310 **3.4. Aerobic CH₄ oxidation in the reservoir**

311 Between 2010 and 2012, the depth integrated aerobic CH₄ oxidation rates ranged between
312 0.05 and 380 mmol m⁻² d⁻¹ at the stations RES1-RES8 (Figure 4). On average, aerobic
313 oxidation was higher in the WW season (55±63 mmol m⁻² d⁻¹) than in the CD (30±46 mmol
314 m⁻² d⁻¹) and WD (36±32 mmol m⁻² d⁻¹) seasons and it was not statistically different for the
315 three years. In the WD season, aerobic CH₄ oxidation was on average twice higher in 2010
316 than for the two following years whereas in the CD season, the highest aerobic oxidation rate
317 was observed in 2012.

318 **3.5. Spatial and seasonal variability of surface CH₄ concentration and diffusive fluxes** 319 **at the reservoir surface (RES1-RES8)**

320 The surface concentrations at the stations RES1-8 ranged from 0.02 to 150 μmol L⁻¹ and were
321 2.0±10.5 μmol L⁻¹ (median = 0.9), 1.5±5.5 μmol L⁻¹ (median = 0.4) and 3.4±14.7 μmol L⁻¹
322 (median = 0.2) on average for the CD, WD and WW season, respectively. The surface
323 concentration followed a loglogistic distribution, which indicates the existence of extremely
324 high values. This is confirmed by the fact that the skewness of the time series of the log of the
325 CH₄ concentrations for all stations is positive (Figure S3), especially at the stations RES1,
326 RES3 and RES7 for which the skewness is >1. Over the course of the three and a half year of
327 survey, the surface concentrations were not statistically different between all stations and no
328 statistically significant seasonal variations were observed because of the occurrence of
329 sporadic events at all season (Figure S2a). The normalized distribution of concentrations (in
330 log) according to seasons (Figure 5) indicates that these high concentrations were observed
331 without any clear seasonal trend at the station RES1, RES5 and RES6 (<1 up to 150 μmol L⁻¹

332 ¹). At the stations RES2 and RES3, the concentrations up to 128 $\mu\text{mol L}^{-1}$ were mostly
333 observed in the CD season when the reservoir overturns. At the station RES4 located at the
334 Nam Xot and Nam Theun confluence and at the stations RES7 and RES8 both located in the
335 inflow region of the Nam Theun River, the high surface concentrations (up to 64.60 $\mu\text{mol L}^{-1}$)
336 were mostly observed during the WW season when the reservoir undergoes sporadic
337 destratification. The auto-correlation function of the time series of the log of the surface CH_4
338 concentrations and diffusive fluxes at the stations RES1-8 indicated that at all stations (except
339 RES1) have a memory effect of 30 to 40 days (Figure S1). This implies that with a sampling
340 frequency of 15 days, we captured most of the changes in the surface CH_4 concentrations. At
341 the station RES1, the changes in CH_4 concentrations are faster than at other stations and
342 would have deserved a monitoring with a frequency higher than 15 days.

343 During the monitoring at RES1-RES8 stations, the average diffusive flux was 2.8 ± 12.2
344 $\text{mmol m}^{-2} \text{d}^{-1}$ ranging from 0.01 to 201.86 $\text{mmol m}^{-2} \text{d}^{-1}$ without any clear interannual and
345 seasonal trends (Figure S2b). As for the concentrations, flux data followed a loglogistic
346 distribution. The median flux in the WD season is 40 to 80% higher than the median in the
347 WW and CD season, respectively. However, the average fluxes in the WW and CD season are
348 30% higher than in the WD season (Table 2). This confirms the presence of extremely high
349 values during WD and CD seasons, as expected from the surface concentrations. All seasons
350 together, around 7% of the diffusive fluxes that we observed were higher than 5 $\text{mmol m}^{-2} \text{d}^{-1}$
351 which corresponds to extremely high diffusive fluxes in comparison with data from the
352 literature for reservoirs and lakes (Bastviken et al., 2008;Barros et al., 2011). The median and
353 average of these extreme fluxes higher than 5 $\text{mmol m}^{-2} \text{d}^{-1}$ were 2 times higher in the WW
354 and CD seasons than in the WD season (Table 2).

355 At NT2, diffusive CH_4 fluxes covered the whole range of fluxes reported for tropical
356 reservoirs, depending on the season. Most of the fluxes at the NT2R Reservoir were around
357 one order of magnitude lower than the ones at Petit Saut Reservoir (French Guiana) just after
358 the impoundment (Galy-Lacaux et al., 1997), and in the same order of magnitude as reported
359 for reservoirs older by 10 to 18 years (Abril et al., 2005;Guerin et al., 2006;Kemenes et al.,
360 2007;Chanudet et al., 2011). However, some diffusive fluxes at the stations RES1-8 in the
361 WW and the CD seasons (up to 202 $\text{mmol m}^{-2} \text{d}^{-1}$) are among the highest ever reported at the
362 surface of a hydroelectric reservoir or a lake (Bastviken et al., 2011;Barros et al., 2011) and
363 rivers downstream of dams (Abril et al., 2005;Guerin et al., 2006;Deshmukh et al., 2015).

364 **3.6. Surface methane concentrations and diffusive fluxes at the water intake (RES9)**

365 After the commissioning of the reservoir (Julian day 450), the concentrations at the stations
366 RES9 (Figure 6a) located at the water intake were up to 30 times higher than at any other
367 stations that is $36.6 \pm 35.8 \mu\text{mol L}^{-1}$ (median = 24.3), $37.6 \pm 67.0 \mu\text{mol L}^{-1}$ (median = 0.9) and
368 $1.0 \pm 1.7 \mu\text{mol L}^{-1}$ (median = 0.3) in the WD, WW and CD season, respectively. The surface
369 concentrations at RES9 were significantly higher in the WD and WW seasons than in the WW
370 and CD seasons ($p = 0.0002$ and Figure 6a). The highest concentration was observed each
371 year at the end of the WD season-beginning of the WW season in between June and August.
372 These maxima decreased from $215 \mu\text{mol L}^{-1}$ in August 2010 to $87 \mu\text{mol L}^{-1}$ in June 2012.

373 The diffusive fluxes ranged between 0.03 and $605.38 \text{ mmol m}^{-2} \text{ d}^{-1}$ (Figure 6b and Table 2).
374 On average, the CH_4 diffusive fluxes at RES9 were two to forty times higher than at the other
375 stations in the CD, WD and WW season. Diffusive fluxes at this station are usually higher
376 than $10 \text{ mmol m}^{-2} \text{ d}^{-1}$ from April to July that corresponds to the WD season and the very
377 beginning of the WW season. In 2010, diffusive fluxes were on average 241 ± 219 and $239 \pm$
378 $228 \text{ mmol m}^{-2} \text{ d}^{-1}$ respectively for the WD and WW seasons. In 2011 and 2012, the fluxes
379 dropped down by a factor of two in the WD season ($112 \pm 110 \text{ mmol m}^{-2} \text{ d}^{-1}$) and almost by a
380 factor of forty in the WW season ($6.8 \pm 14.4 \text{ mmol m}^{-2} \text{ d}^{-1}$). Overall, emissions at RES9
381 decreased by a factor of two between 2010 and 2012.

382 At the water intake, CH_4 diffusive fluxes during the transition between the WD and WW
383 seasons (up to $600 \text{ mmol m}^{-2} \text{ d}^{-1}$) are the highest reported at the surface of an aquatic
384 ecosystem (Abril et al., 2005;Guerin et al., 2006;Bastviken et al., 2011;Barros et al.,
385 2011;Deshmukh et al., 2015).

386 **4. Discussion**

387 **4.1. CH_4 dynamic in the reservoir water column**

388 The gradual decrease of the CH_4 concentration from the anoxic bottom water column to the
389 metalimnion and the sharp decrease around the oxicleine in the metalimnion (Figure 2) is
390 typical in reservoirs and lakes where CH_4 is produced in anoxic sediments and flooded soils
391 (Guerin et al., 2008;Sobek et al., 2012;Maeck et al., 2013), and where most of it is oxidized at
392 the oxic-anoxic interface (Bedard and Knowles, 1997;Bastviken et al., 2002;Guerin and Abril,
393 2007;Deshmukh et al., 2015).

394 CH₄ concentrations and storage increase concomitantly with the surface water temperature
395 and the establishment of the thermal stratification during the WD season and peak at the end
396 of the WD season-beginning of the WW season (Figure 2 and 3). During the WW season,
397 CH₄ concentrations and storage decrease slowly (Figure 3) while aerobic methane oxidation
398 reaches its maximum (Figure 4). When the reservoir overturns at the beginning of the CD
399 season, the CH₄ hypolimnic concentrations and storage reach their minima (Figure 3). The
400 overturn favours the penetration of oxygen down to the bottom (Figure 2 and 3b). The sharp
401 decrease of the CH₄ concentrations and CH₄ storage during this period is expected to result
402 from sudden outgassing (Section 4.2) together with an enhancement of the aerobic CH₄
403 oxidation as already observed in lakes that overturn (Utsumi et al., 1998b;Utsumi et al.,
404 1998a;Kankaala et al., 2007;López Bellido et al., 2009;Schubert et al., 2010;Schubert et al.,
405 2012;Fernández et al., 2014). A large increase of the aerobic methane oxidation was only
406 observed in the CD season in the dry year 2012 (Figure 4) because the amount of hypolimnic
407 CH₄ to be oxidized at the beginning of the CD season was still high in the water column
408 (Figure 3c,d).

409 As the reservoir overturns during the period over which the water residence time is the longest
410 in the reservoir, the temporal evolution of the concentrations is anti-correlated with the
411 residence time (Figure 3c,d). The seasonal dynamics of the CH₄ in the monomictic NT2R
412 differs from permanently stratified reservoirs like Petit Saut Reservoir where CH₄
413 concentration increased with retention time (Abril et al., 2005). However, at the annual scale
414 the water residence time has a strong influence on CH₄ concentration and storage in the
415 reservoir. Before the reservoir was commissioned (April 2010), the water residence time was
416 up to 4 years and the CH₄ storage was up to four times higher than in 2011 and 2012 (Figure
417 3d). Although a decrease of concentration and storage with the age of the reservoir was
418 expected (Abril et al., 2005), the storage in the dry year 2012 was twice higher than in the wet
419 year 2011 due to an increase of the water residence time by 25% between 2011 and 2012. In
420 wet years like 2011, the thermal stratification is weaker than in dry years since the warming of
421 surface water is less efficient and the high water inputs alters the stability of the reservoir
422 thermal stratification as shown by the sharper decrease and the larger range of ΔT in 2011
423 than in 2012 (Figure 3a). As a consequence, the oxygen diffusion to the hypolimnion was
424 higher in 2011 than in 2012 (Figure 3b) and it enhanced aerobic methane oxidation by 20% in
425 the water column in the WW season in 2011 as compared to 2012 (Figure 4). It therefore
426 suggests that the hydrology affects both the thermal stratification and the hypolimnic storage

427 of CH₄ in reservoirs, indirectly controls aerobic methane oxidation, and ultimately influences
428 emissions.

429 **4.2. Hot moments of emissions during sporadic destratification and reservoir overturn**

430 The figure 7 illustrates the evolution of the diffusive fluxes, the stratification index (ΔT), the
431 CH₄ storage and the aerobic CH₄ oxidation at the stations RES1, RES3, RES7 and RES8.
432 These four stations were selected for their contrasting skewness (Figure S3) which gives an
433 indication on the occurrence of extreme events and the facts that they are representative for all
434 station characteristics (Table 1). It shows that the large bursts of CH₄ (from 5 up to 200 mmol
435 m⁻² d⁻¹) always occurred when ΔT decreased sharply ($>4^{\circ}\text{C}$, Figure 7a,d,g,j) and are usually
436 followed by a sharp decrease of the CH₄ storage in the water column (Figure 7b,e,h,k). These
437 hot moments of emissions occurred mostly in the CD at the stations RES1 and RES3 whereas
438 it was in the WW season at the stations RES7 and RES8 (Figure 7). In the WD season,
439 diffusive fluxes gradually increased together with the CH₄ storage in the water column
440 (Figure 7a,d,g,j) and they remained always lower than 20 mmol m⁻² d⁻¹. These sporadic high
441 fluxes occurred in the WD season at RES3, RES7 and RES8 (Figure 7d,g,j). They are usually
442 associated with ΔT variations lower than 2°C and the CH₄ storage decrease that is associated
443 with these fluxes is not as sharp as the one observed in the CD and WW season (Figure
444 7e,h,k).

445 We therefore confirm the occurrence of hot moments of emissions during the reservoir
446 overturn in the CD season as already observed in lakes that overturn in temperate regions
447 (Kankaala et al., 2007;López Bellido et al., 2009;Schubert et al., 2010;Schubert et al.,
448 2012;Fernández et al., 2014). The highest emissions determined at NT2R are one order of
449 magnitude higher than previously reported outgassing during overturn and they occur mostly
450 in the section of the reservoir that has the longest water residence time (RES1-3, Table 1) and
451 the largest CH₄ storage (Figure 7b,e,h,k). This suggests that the impact of reservoir overturn
452 can be very critical for the whole-reservoir CH₄ budget in tropical hydroelectric reservoirs and
453 especially in young ones where hypolimnic concentration could reach up to 1000 $\mu\text{mol L}^{-1}$.
454 Hot moments of emissions also occur during sporadic destratifications in the WW season in
455 the inflow region (RES4 and RES6-8) where the inflow of cool water from the watershed
456 might disrupt the thermal stratification in reservoirs. This is contrasting with the observations
457 in older reservoir than NT2R where high emissions from the inflow region were recently
458 attributed to an enhancement of CH₄ production fuelled by the sedimentation of organic

459 matter from the watershed (Musenze et al., 2014). The high emissions in the WD seasons
460 were associated with early rains and associated high winds that occur sometimes in the last
461 fifteen days of May. This shows that a moderate erosion of the stratification when hypolimnic
462 CH₄ concentrations are high could enhance vertical transport of CH₄ toward the surface and
463 emissions to the atmosphere. Basically, this intense monitoring shows that spatial and
464 temporal variations of CH₄ emissions are largely controlled by the hydrodynamics of the
465 reservoir with extreme emissions occurring mostly in the inflow region during the wet season
466 and mostly in area remotely located from the inflow zone and the riverbed during reservoir
467 overturns in the CD season. Even if less frequent, moderate erosion of the stable and steep
468 thermal stratification during warm seasons, could also lead to high emissions.

469 The evolution of depth-integrated aerobic CH₄ oxidation is not clearly related with the
470 reservoir overturns and the CH₄ burst (Figure 7). Significant increases in the aerobic CH₄
471 oxidation occurred mostly during the first half of the WD season when the stratification was
472 unstable and at the very beginning of the destratification in the WW, when ΔT started to
473 decrease. The oxidation could reach high values (up to 380 mmol m⁻² d⁻¹) during these two
474 periods since the yield of CH₄ in the water column to sustain the activity of methanotrophs is
475 higher than in the CD season when the reservoir overturns. It shows that in reservoirs or lakes
476 like NT2R that destratify progressively before the overturn, there is no substantial increase of
477 the CH₄ oxidation when the water body overturns as it could be observed in lakes that
478 overturn within a few days (Kankaala et al., 2007). In addition, the contribution of CH₄
479 oxidation to the total loss of CH₄ (sum of diffusion and oxidation) in the WD and WW
480 seasons was 90-95% during the entire monitoring whereas it was 85% in the CD season.
481 During overturns, a significant amount of CH₄ is oxidized (Utsumi et al., 1998a; Utsumi et al.,
482 1998b; Kankaala et al., 2007; Schubert et al., 2012) but it also indicates that the removal of
483 CH₄ during overturn is not as efficient as during seasons with a well established thermal
484 stratification.

485 During the periods with major loss in the CH₄ storage with concomitant CH₄ burst, we
486 compared the change in the yield of CH₄ with the sum of emissions and oxidation. Most of
487 the time, the emissions alone and/or the sum of emissions and oxidation were significantly
488 higher than the amount of CH₄ that was lost from the water column. At the Pääjärvi Lake in
489 Finland (López Bellido et al., 2009), the fact that measured or calculated emissions exceed the
490 loss of CH₄ in the water column was attributed to a probable underestimation of the CH₄

491 storage in the lake by under-sampling the shallow area of the lake. In this study, emissions,
492 storage and oxidation were estimated at the same stations, avoiding such sampling artefacts.
493 Therefore, it suggests that CH₄ is provided by lateral transport or by production in the flooded
494 soil and biomass (Guerin et al., 2008) at a higher rate than the total loss of CH₄ from the water
495 column by emissions and oxidation. This hypothesis could only be verified by a full CH₄
496 mass balance including production and total emissions from the reservoir, which is beyond
497 the scope of this article.

498 **4.3. Hot spot of emissions at the water intake (RES9)**

499 After the commissioning of the reservoir, the temperature and the oxygen and CH₄
500 concentrations were constant from the surface to the bottom of the reservoir at the vicinity of
501 the water intake. On the basis of physical modelling and measurements of water current
502 velocities (Chanudet et al., 2012), the vertical mixing at this station was attributed to the water
503 withdrawal at the intake generating turbulence and water currents over a surface area of 3
504 km². At this station, CH₄-rich water from the reservoir hypolimnion reached the surface and
505 led to diffusive fluxes up to 600 mmol m⁻² d⁻¹ in the WD-WW seasons (Figure 6b) whereas
506 fluxes are 3 orders of magnitude lower in the CD season. To the best of our knowledge, this is
507 the first time that a hotspot of emissions is reported upstream of a dam or an intake bringing
508 water to the turbines. At NT2, the intake is located at the bottom of a narrow and shallow
509 channel (depth =9-20 m) on the side of the reservoir. This design enhances horizontal water
510 current velocities, the vertical mixing and therefore the emissions. The existence of such a
511 hotspot at other reservoirs might be highly dependant on the design of the water intake (depth
512 among other parameters) and its effect on the hydrodynamics of the reservoir water column.

513 **4.4. Estimation of total diffusive fluxes from the reservoir**

514 Yearly emissions by diffusive fluxes peaked at more than 9 Gg(CH₄) in 2010 when the
515 reservoir was commissioned and they decreased down to ≈ 5 Gg(CH₄) in 2011 and 2012
516 (Figure 8a and Table 3). Yearly integrated at the whole reservoir surface, these emissions
517 correspond to diffusive fluxes of 1.5 to 4 mmol m⁻² d⁻¹. These emissions are significantly
518 lower than diffusive fluxes measured at the Petit Saut Reservoir during the first two years
519 after flooding but similar to those determined in the following years (Abril et al., 2005) and
520 values reported for diffusive fluxes from tropical reservoirs in Barros et al. (2011). In absence
521 of the extreme emissions (both hotspots and hot moments), diffusive emissions from NT2R

522 would have been one order of magnitude lower than emissions from tropical reservoirs as
523 expected from the lower flooded biomass compare to Amazonian reservoirs (Descloux et al.,
524 2011). Due to the specific dynamic of diffusive fluxes at NT2R, diffusion at the reservoir
525 surface contribute 18 to 27% of total emissions (Table 3) that is significantly higher than at
526 other reservoirs tropical reservoirs where it was measured (See Deshmukh et al., 2015 for a
527 detailed discussion).

528 Most of the increase of CH₄ emissions by diffusive fluxes from 4 to 9 Gg(CH₄) between 2009
529 and 2010 is due to very significant emissions of 2-3 Gg(CH₄) at the water intake (Figure 8a).
530 This outgassing of CH₄ was triggered by the vertical mixing generated by the withdrawal of
531 water from the reservoir to the turbines. Although the area under the influence of the water
532 intake is less than 1% of the total area of the reservoir, emissions at the water intake
533 contributed between 13 and 25% of total diffusive emissions and 4 to 10 % if considering
534 both ebullition and diffusion (Table 3). It is worth to note that emissions at this site are only
535 significant within 3-5 month per year at the end of the WD season-beginning of the WW
536 season when the storage of CH₄ reach its maximum in the reservoir (Figure 8b). This new
537 hotspot equals 20 to 40% of downstream emissions and contributes between 4 and 7% of total
538 emissions from the NT2 reservoir surface when including ebullition and downstream
539 emissions (Table 3 and Deshmukh et al. (2015)). Very localized perturbation of the
540 hydrodynamics, especially in lakes or reservoirs with CH₄-rich hypolimnion, can generate
541 hotspots of emissions contributing significantly to the total emissions from a given ecosystem.
542 These hotspots could be found upstream of dams and water intake in reservoirs but also
543 around aeration stations based on air injection or artificial mixing that could be used for
544 improving water quality in water bodies (Wüest et al., 1992).

545 The contribution of extreme diffusive fluxes (> 5 up to $200 \text{ mmol m}^{-2} \text{ d}^{-1}$) to total emission by
546 diffusion range from 30 to 50% on a yearly basis (Figure 8a) and from 40 up to 70% on a
547 monthly basis (Figure 8b) although these hot moments represent less than 10% of the
548 observations during the monitoring. In the literature, the statistical distribution of CH₄
549 emissions dataset always follows heavy-tailed and right skewed distribution like the log-
550 normal, the Generalized Pareto Distribution (Windsor et al., 1992;Czepiel et al., 1993;Ramos
551 et al., 2006;DelSontro et al., 2011) or loglogistic (this study) which indicates that CH₄
552 emissions are always characterized by high episodic fluxes. The quantification of emissions
553 thus requires the highest spatial and temporal resolutions in order to capture as many hot
554 moments as possible. At a single station, extreme emission events never lasted more than 2

555 months (3 consecutive sampling dates) and probably lasted less than 15 days most of the time
556 (Figure 7). The auto-correlation function of the concentration time series indicate that a
557 minimum sampling frequency of 1 month is required in this monomictic reservoirs for an
558 accurate description of the change in the surface concentrations and estimation of the
559 emissions (Figure S1). A lower temporal resolution can significantly affect (positively or
560 negatively) the emissions factors of non-permanently stratified freshwater reservoirs. This is
561 particularly critical in the inflow regions when water inputs from the watershed increase in the
562 rainy season in all reservoirs and at the beginning of the overturn in regions of the world
563 where reservoirs are not permanently stratified like in Asia (Chanudet et al., 2011) which
564 concentrate 60% of the worldwide hydroelectric reservoirs (Kumar et al., 2011).

565 **5. Conclusion**

566 The fortnightly monitoring of CH₄ diffusive emissions at nine stations revealed complex
567 temporal and spatial variations that could hardly been characterized by seasonal sampling.
568 The highest emissions occur sporadically during hot moments in the rainy season and when
569 the reservoir overturns. In the rainy season, they mostly occur in the inflow region because the
570 increase of the discharge of cool water from the reservoir tributaries contributes to sporadic
571 thermal destratification. During the reservoir overturn, extreme emissions occur mostly in
572 area remotely located from the inflows and outflows that are supposed to have the highest
573 water residence time. It shows that diffusive emissions can be sporadically as high as
574 ebullition and that these hot moments could contribute very significantly to the total emissions
575 from natural aquatic ecosystems and reservoirs. Our results showing that a monthly frequency
576 monitoring is the minimum required to capture all emissions is probably not applicable to
577 every aquatic ecosystem. However, it suggests that quantification of emissions based on 2-4
578 campaigns in a year might significantly affect emissions factors and carbon budgets of
579 ecosystems under study.

580 We also identified a new hotspot of emissions upstream of the water intake resulting from the
581 artificial destratification of the water column due to horizontal and vertical mixing generated
582 by the water withdrawal. In the case of the NT2R, emissions from this site contribute up to
583 25% of total diffusive emissions over less than 1% of the total reservoir area. We highly
584 recommend measurements of diffusive fluxes around water intakes (immediately upstream of
585 dams, typically) in order to evaluate if such results can be generalized.

586 **Acknowledgements**

587 The authors thank everyone who contributed to the NT2 monitoring programme, especially
588 the Nam Theun 2 Power Company (NTPC) and Electricité de France (EDF) for providing
589 financial, technical and logistic support. We are also grateful to the Aquatic Environment
590 Laboratory of the Nam Theun 2 Power Company whose Shareholders are EDF, Lao Holding
591 State Enterprise and Electricity Generating Public Company Limited of Thailand. CD
592 benefited from a PhD grant by EDF.

593

594 **References**

- 595 Abril, G., Guerin, F., Richard, S., Delmas, R., Galy-Lacaux, C., Gosse, P., Tremblay, A.,
596 Varfalvy, L., Dos Santos, M. A., and Matvienko, B.: Carbon dioxide and methane emissions
597 and the carbon budget of a 10-year old tropical reservoir (Petit Saut, French Guiana), *Glob.*
598 *Biogeochem. Cycle*, 19, 10.1029/2005gb002457, 2005.
- 599 Abril, G., Commarieu, M.-V., and Guerin, F.: Enhanced methane oxidation in an estuarine
600 turbidity maximum, *Limnology and Oceanography*, 52, 470-475, 2007.
- 601 Barros, N., Cole, J. J., Tranvik, L. J., Prairie, Y. T., Bastviken, D., Huszar, V. L. M., del
602 Giorgio, P., and Roland, F.: Carbon emission from hydroelectric reservoirs linked to reservoir
603 age and latitude, *Nature Geosci*, 4, 593-596, 2011.
- 604 Bastviken, D., Ejlertsson, J., and Tranvik, L.: Measurement of methane oxidation in lakes: A
605 comparison of methods, *Environmental Science & Technology*, 36, 3354-3361,
606 10.1021/es010311p, 2002.
- 607 Bastviken, D., Cole, J. J., Pace, M. L., and Van de Bogert, M. C.: Fates of methane from
608 different lake habitats: Connecting whole-lake budgets and CH₄ emissions, *Journal of*
609 *Geophysical Research-Biogeosciences*, 113, G02024
610 10.1029/2007jg000608, 2008.
- 611 Bastviken, D., Tranvik, L. J., Downing, J. A., Crill, P. M., and Enrich-Prast, A.: Freshwater
612 Methane Emissions Offset the Continental Carbon Sink, *Science*, 331, 50,
613 10.1126/science.1196808, 2011.
- 614 Bedard, C., and Knowles, R.: Some properties of methane oxidation in a thermally stratified
615 lake, *Canadian Journal of Fisheries and Aquatic Sciences*, 54, 1639-1645, 1997.
- 616 Borges, A. V., Delille, B., Schiettecatte, L. S., Gazeau, F., Abril, G., and Frankignoulle, M.:
617 Gas transfer velocities of CO₂ in three European estuaries (Randers Fjord, Scheldt, and
618 Thames), *Limnology and Oceanography*, 49, 1630-1641, 2004.
- 619 Chanudet, V., Descloux, S., Harby, A., Sundt, H., Hansen, B. H., Brakstad, O., Serca, D., and
620 Guerin, F.: Gross CO₂ and CH₄ emissions from the Nam Ngum and Nam Leuk sub-tropical
621 reservoirs in Lao PDR, *Science of the Total Environment*, 409, 5382-5391,
622 10.1016/j.scitotenv.2011.09.018, 2011.
- 623 Chanudet, V., Fabre, V., and van der Kaaij, T.: Application of a three-dimensional
624 hydrodynamic model to the Nam Theun 2 Reservoir (Lao PDR), *Journal of Great Lakes*
625 *Research*, 38, 260-269, <http://dx.doi.org/10.1016/j.jglr.2012.01.008>, 2012.
- 626 Chen, H., Wu, Y., Yuan, X., Gao, Y., Wu, N., and Zhu, D.: Methane emissions from newly
627 created marshes in the drawdown area of the Three Gorges Reservoir, *J. Geophys. Res.*, 114,
628 D18301, doi:10.1029/2009JD012410, 2009.
- 629 Chen, H., Yuan, X., Chen, Z., Wu, Y., Liu, X., Zhu, D., Wu, N., Zhu, Q. a., Peng, C., and Li,
630 W.: Methane emissions from the surface of the Three Gorges Reservoir, *J. Geophys. Res.*,
631 116, D21306, 10.1029/2011jd016244, 2011.
- 632 Czepiel, P. M., Crill, P. M., and Harriss, R. C.: Methane emissions from municipal
633 wastewater treatment processes, *Environmental Science & Technology*, 27, 2472-2477,
634 10.1021/es00048a025, 1993.
- 635 Delignette-Muller, M. L., Dutang, C., Pouillot, R., and Denis, J.-B.: An R Package for Fitting
636 Distributions, 1.0-4, 2015
- 637 DelSontro, T., McGinnis, D. F., Sobek, S., Ostrovsky, I., and Wehrli, B.: Extreme Methane
638 Emissions from a Swiss Hydropower Reservoir: Contribution from Bubbling Sediments,
639 *Environmental Science & Technology*, 44, 2419-2425, 10.1021/es9031369, 2010.
- 640 DelSontro, T., Kunz, M. J., Kempter, T., Wüest, A., Wehrli, B., and Senn, D. B.: Spatial
641 Heterogeneity of Methane Ebullition in a Large Tropical Reservoir, *Environmental Science &*
642 *Technology*, 45, 9866-9873, 10.1021/es2005545, 2011.

643 Descloux, S., Chanudet, V., Poilvé, H., and Grégoire, A.: Co-assessment of biomass and soil
644 organic carbon stocks in a future reservoir area located in Southeast Asia, *Environmental*
645 *Monitoring and Assessment*, 173, 723-741, 10.1007/s10661-010-1418-3, 2011.

646 Descloux, S., Guedant, P., Phommachanh, D., and Luthi, R.: Main features of the Nam Theun
647 2 hydroelectric project (Lao PDR) and the associated environmental monitoring programmes,
648 *Hydroécol. Appl.*, 10.1051/hydro/2014005 2014, 2014.

649 Deshmukh, C., Serca, D., Delon, C., Tardif, R., Demarty, M., Jarnot, C., Meyerfeld, Y.,
650 Chanudet, V., Guedant, P., Rode, W., Descloux, S., and Guerin, F.: Physical controls on CH₄
651 emissions from a newly flooded subtropical freshwater hydroelectric reservoir: Nam Theun 2,
652 *Biogeosciences*, 11, 4251-4269, 10.5194/bg-11-4251-2014, 2014.

653 Deshmukh, C., Guérin, F., Pighini, S., Vongkhamsao, A., Guédant, P., Rode, W., Chanudet,
654 V., Descloux, S., Godon, A., and Serça, D.: Low methane (CH₄) emissions downstream of a
655 newly flooded subtropical hydroelectric reservoir (Nam Theun 2, Lao PDR), *Biogeoscience*
656 *Discussion*, 12, 11313-11347, 10.5194/bgd-12-11313-2015, 2015.

657 Fernández, J. E., Peeters, F., and Hofmann, H.: Importance of the Autumn Overturn and
658 Anoxic Conditions in the Hypolimnion for the Annual Methane Emissions from a Temperate
659 Lake, *Environmental Science & Technology*, 48, 7297-7304, 10.1021/es4056164, 2014.

660 Galy-Lacaux, C., Delmas, R., Jambert, C., Dumestre, J. F., Labroue, L., Richard, S., and
661 Gosse, P.: Gaseous emissions and oxygen consumption in hydroelectric dams: A case study in
662 French Guyana, *Glob. Biogeochem. Cycle*, 11, 471-483, 1997.

663 Gross, J., and Ligges, U.: Tests for Normality (Nortest), 1.04-4, 2015

664 Guerin, F., Abril, G., Richard, S., Burban, B., Reynouard, C., Seyler, P., and Delmas, R.:
665 Methane and carbon dioxide emissions from tropical reservoirs: Significance of downstream
666 rivers, *Geophysical Research Letters*, 33, 10.1029/2006gl027929, 2006.

667 Guerin, F., and Abril, G.: Significance of pelagic aerobic methane oxidation in the methane
668 and carbon budget of a tropical reservoir, *Journal of Geophysical Research-Biogeosciences*,
669 112, 10.1029/2006jg000393, 2007.

670 Guerin, F., Abril, G., Serca, D., Delon, C., Richard, S., Delmas, R., Tremblay, A., and
671 Varfalvy, L.: Gas transfer velocities of CO₂ and CH₄ in a tropical reservoir and its river
672 downstream, *Journal of Marine Systems*, 66, 161-172, 10.1016/j.jmarsys.2006.03.019, 2007.

673 Guerin, F., Abril, G., de Junet, A., and Bonnet, M.-P.: Anaerobic decomposition of tropical
674 soils and plant material: Implication for the CO₂ and CH₄ budget of the Petit Saut Reservoir,
675 *Applied Geochemistry*, 23, 2272-2283, 10.1016/j.apgeochem.2008.04.001, 2008.

676 Jahne, B., Munnich, K. O., Bosinger, R., Dutzi, A., Huber, W., and Libner, P.: On the
677 parameters influencing air-water gas-exchange, *J. Geophys. Res.-Oceans*, 92, 1937-1949,
678 1987.

679 Kankaala, P., Taipale, S., Nykanen, H., and Jones, R. I.: Oxidation, efflux, and isotopic
680 fractionation of methane during autumnal turnover in a polyhumic, boreal lake, *Journal of*
681 *Geophysical Research-Biogeosciences*, 112, G02003
682 10.1029/2006jg000336, 2007.

683 Kemenes, A., Forsberg, B. R., and Melack, J. M.: Methane release below a tropical
684 hydroelectric dam, *Geophysical Research Letters*, 34, L12809 10.1029/2007gl029479, 2007.

685 Kumar, A., Schei, T., Ahenkorah, A., Rodriguez, R. C., Devernay, J.-M., Freitas, M., Hall, D.,
686 Killingtveit, A., and Liu, Z.: *Hydropower*, Cambridge, United Kingdom and New York, NY,
687 USA., 437-496, 2011.

688 López Bellido, J., Tulonen, T., Kankaala, P., and Ojala, A.: CO₂ and CH₄ fluxes during
689 spring and autumn mixing periods in a boreal lake (Pääjärvi, southern Finland), *Journal of*
690 *Geophysical Research: Biogeosciences*, 114, G04007, 10.1029/2009JG000923, 2009.

691 MacIntyre, S., Jonsson, A., Jansson, M., Aberg, J., Turney, D. E., and Miller, S. D.: Buoyancy
692 flux, turbulence, and the gas transfer coefficient in a stratified lake, *Geophysical Research*
693 *Letters*, 37, L24604, 10.1029/2010GL044164, 2010.

694 Maeck, A., DelSontro, T., McGinnis, D. F., Fischer, H., Flury, S., Schmidt, M., Fietzek, P.,
695 and Lorke, A.: Sediment Trapping by Dams Creates Methane Emission Hot Spots,
696 *Environmental Science & Technology*, 47, 8130-8137, 10.1021/es4003907, 2013.

697 McClain, M. E., Boyer, E. W., Dent, C. L., Gergel, S. E., Grimm, N. B., Groffman, P. M.,
698 Hart, S. C., Harvey, J. W., Johnston, C. A., Mayorga, E., McDowell, W. H., and Pinay, G.:
699 Biogeochemical hot spots and hot moments at the interface of terrestrial and aquatic
700 ecosystems, *Ecosystems*, 6, 301-312, 10.1007/s10021-003-0161-9, 2003.

701 Musenze, R. S., Grinham, A., Werner, U., Gale, D., Sturm, K., Udy, J., and Yuan, Z.:
702 Assessing the Spatial and Temporal Variability of Diffusive Methane and Nitrous Oxide
703 Emissions from Subtropical Freshwater Reservoirs, *Environmental Science & Technology*,
704 48, 14499-14507, 10.1021/es505324h, 2014.

705 NTPC: Environmental Assessment and Management Plan - Nam Theun 2 Hydroelectric
706 Project. Nam Theun 2 Power Company, NTPC (Nam Theun 2 Power Company), Vientiane,
707 212, 2005.

708 Pacheco, F. S., Soares, M. C. S., Assireu, A. T., Curtarelli, M. P., Roland, F., Abril, G., Stech,
709 J. L., Alvalá, P. C., and Ometto, J. P.: The effects of river inflow and retention time on the
710 spatial heterogeneity of chlorophyll and water-air CO₂ fluxes in a tropical hydropower
711 reservoir, *Biogeosciences*, 12, 147-162, 10.5194/bg-12-147-2015, 2015.

712 R Development Core Team: R: A Language and Environment for Statistical Computing, R
713 Foundation for Statistical Computing, Vienna, Austria, 3-900051-07-0, 2008

714 Ramos, F. M., Lima, I. B. T., Rosa, R. R., Mazzi, E. A., Carvalho, J. o. C., Rasera, M. F. F.
715 L., Ometto, J. P. H. B., Assireu, A. T., and Stech, J. L.: Extreme event dynamics in methane
716 ebullition fluxes from tropical reservoirs, *Geophys. Res. Lett.*, 33, L21404,
717 10.1029/2006gl027943, 2006.

718 Schubert, C., Lucas, F., Durisch-Kaiser, E., Stierli, R., Diem, T., Scheidegger, O., Vazquez,
719 F., and Müller, B.: Oxidation and emission of methane in a monomictic lake (Rotsee,
720 Switzerland), *Aquatic Sciences - Research Across Boundaries*, 72, 455-466, 10.1007/s00027-
721 010-0148-5, 2010.

722 Schubert, C. J., Diem, T., and Eugster, W.: Methane Emissions from a Small Wind Shielded
723 Lake Determined by Eddy Covariance, Flux Chambers, Anchored Funnels, and Boundary
724 Model Calculations: A Comparison, *Environmental Science & Technology*, 46, 4515-4522,
725 10.1021/es203465x, 2012.

726 Sobek, S., DelSontro, T., Wongfun, N., and Wehrli, B.: Extreme organic carbon burial fuels
727 intense methane bubbling in a temperate reservoir, *Geophys. Res. Lett.*, 39, L01401,
728 10.1029/2011gl050144, 2012.

729 St Louis, V. L., Kelly, C. A., Duchemin, E., Rudd, J. W. M., and Rosenberg, D. M.: Reservoir
730 surfaces as sources of greenhouse gases to the atmosphere: A global estimate, *Bioscience*, 50,
731 766-775, 2000.

732 Sturm, K., Yuan, Z., Gibbes, B., Werner, U., and Grinham, A.: Methane and nitrous oxide
733 sources and emissions in a subtropical freshwater reservoir, South East Queensland, Australia,
734 *Biogeosciences*, 11, 5245-5258, 10.5194/bg-11-5245-2014, 2014.

735 Teodoru, C. R., Bastien, J., Bonneville, M.-C., del Giorgio, P. A., Demarty, M., Garneau, M.,
736 Hélie, J.-F., Pelletier, L., Prairie, Y. T., Roulet, N. T., Strachan, I. B., and Tremblay, A.: The
737 net carbon footprint of a newly created boreal hydroelectric reservoir, *Glob. Biogeochem.*
738 *Cycle*, 26, GB2016, 10.1029/2011gb004187, 2012.

739 Utsumi, M., Nojiri, Y., Nakamura, T., Nozawa, T., Otsuki, A., and Seki, H.: Oxidation of
740 dissolved methane in a eutrophic, shallow lake: Lake Kasumigaura, Japan, *Limnology and*
741 *Oceanography*, 43, 471-480, 1998a.
742 Utsumi, M., Nojiri, Y., Nakamura, T., Nozawa, T., Otsuki, A., Takamura, N., Watanabe, M.,
743 and Seki, H.: Dynamics of dissolved methane and methane oxidation in dimictic Lake Nojiri
744 during winter, *Limnology and Oceanography*, 43, 10-17, 1998b.
745 Wanninkhof, R.: Relationship between wind-speed and gas-exchange over the ocean, *J.*
746 *Geophys. Res.-Oceans*, 97, 7373-7382, 1992.
747 Windsor, J., Moore, T. R., and Roulet, N. T.: Episodic fluxes of methane from subarctic fens,
748 *Canadian Journal of Soil Science*, 72, 441-452, doi:10.4141/cjss92-037, 1992.
749 Wüest, A., Brooks, N. H., and Imboden, D. M.: Bubble plume modeling for lake restoration,
750 *Water Resources Research*, 28, 3235-3250, 10.1029/92WR01681, 1992.
751 Yamamoto, S., Alcauskas, J. B., and Crozier, T. E.: Solubility of methane in distilled water
752 and seawater, *Journal of Chemical & Engineering Data*, 21, 78-80, 10.1021/je60068a029,
753 1976.
754 Zheng, H., Zhao, X. J., Zhao, T. Q., Chen, F. L., Xu, W. H., Duan, X. N., Wang, X. K., and
755 Ouyang, Z. Y.: Spatial-temporal variations of methane emissions from the Ertan hydroelectric
756 reservoir in southwest China, *Hydrol. Process.*, 25, 1391-1396, 10.1002/hyp.7903, 2011.
757
758

759
760
761

Table 1: Characteristics of the nine monitoring stations in the Nam Theun 2 Reservoir

Station	Flooded ecosystem ¹	Hydrology	Water residence time ²
RES1	Dense forest	100 m upstream of the Nakai Dam	**
RES2	Dense forest	Thalweg of the Nam Theun River	**
RES3	Dense forest	Embayment	***
RES4	Degraded forest	Confluence Nam Theun-Nam Xot Rivers	**
RES5	Degraded forest	Aside from the main stream	**
RES6	Degraded forest	Thalweg of the Nam Theun River	*
RES7	Swamp	Between inflows and water intake	*
RES8	Agricultural soils	Between inflows and water intake	*
RES9	Civil construction	Water intake	*

762 ¹Descloux et al. (2011)

763 ²Water residence time in arbitrary units, (***) stands for long residence time, (**) for
764 intermediate residence times and (*) for short residence times

765

766
 767
 768
 769

Table 2 : Median, average, ranges and proportion of diffusive fluxes (F_{CH_4}) < 1 and > 5 mmol $m^{-1} d^{-1}$ for three seasons

Station		Warm Dry (WD)	Warm Wet (WW)	Cool Dry (CD)
RES1-RES8	n	212	252	217
	range	0.01-102.59	0.01-201.86	0.01-94.64
	median	1.08	0.64	0.20
	Average \pm SD	2.23 \pm 7.37	3.12 \pm 14.58	3.04 \pm 12.89
	% $F_{CH_4} < 1$	48%	63%	86%
	% $F_{CH_4} > 5$	6.6%	7.5%	7.4%
	Mediane $F > 5$	10.67	13.80	23.75
	Average $F > 5$	16.69 \pm 25.04	30.23 \pm 45.99	36.45 \pm 33.19
RES9	n	39	45	36
	range	0.24-342.00	0.03-605.38	0.07-17.62
	median	40.81	1.23	0.48
	average \pm SD	83.33 \pm 15.57	78.58 \pm 24.73	2.21 \pm 0.69

770
 771

772 Table 3: Methane emissions from the Nam Theun 2 Reservoir between 2009 and 2012.

Gg(CH ₄) year ⁻¹	2009	2010	2011	2012
Emission from reservoir				
Diffusion at RES9 only	0.02±0.01	2.33±0.21	0.86±0.12	0.66±0.11
Total diffusion	4.45±1.01	9.34±2.32	3.71±0.81	4.95±1.09
Contribution of RES9 to diffusion (%)	0.4	24.9	23.2	13.3
Ebullition ¹	11.21±0.16	14.39±0.11	14.68±0.10	12.29±0.09
Total emissions from reservoir	15.66±1.02	23.73±2.32	18.39±0.82	17.25±1.09
Contribution of RES9 (%)	0.1	9.8	4.7	3.8
Total downstream emissions²	7.79±0.90	10.73±0.83	2.29±0.41	2.00±0.32
Total emissions (reservoir + downstream)	23.45±1.36	34.46±2.46	20.67±0.92	19.24±1.14
Contribution of diffusion to total emission	19%	27%	18%	26%
Contribution of RES9 to total (%)	<0.1	6.8	4.2	3.4

773 ¹Deshmukh et al. (2014)

774 ²Deshmukh et al. (2015)

775

776

777
778 Figure captions

779
780 Figure 1: Map of the sampling stations and civil structures at the Nam Theun 2 Reservoir
781 (Lao PDR).

782
783 Figure 2: Vertical profiles of temperature ($^{\circ}\text{C}$), oxygen ($\mu\text{mol L}^{-1}$) and methane ($\mu\text{mol L}^{-1}$) at
784 the stations RES1, RES3, RES7, RES8 and RES9 in the Nam Theun 2 Reservoir.
785 Representative profile of the years 2010 (circle), 2011 (square) and 2012 (triangle) are given
786 for each seasons: cool dry in blue, warm dry in red, and warm wet in grey.

787
788 Figure 3: (a) Stratification index (ΔT , see text), (b) O_2 concentration in the hypolimnion
789 ($\mu\text{mol L}^{-1}$), (c) CH_4 concentration in the hypolimnion ($\mu\text{mol L}^{-1}$) and (d) CH_4 storage in the
790 water column ($\text{Gg}(\text{CH}_4) \text{ month}^{-1}$, bars) and water residence time (days, black line with circles)
791 in the Nam Theun 2 Reservoir (Lao PDR) between 2009 and 2012. The red, grey and blue
792 colours indicate the warm dry (WD), warm wet (WW) and cool dry (CD) seasons,
793 respectively. For the panels (a), (b) and (c), the boxes show the median and the interquartile
794 range, the whiskers denote the full range of values and the plus sign (+) denotes the mean.

795
796 Figure 4: Seasonal variations between 2010 and 2012 of the depth-integrated aerobic CH_4
797 oxidation ($\text{mmol m}^{-2} \text{ d}^{-1}$) at the stations RES1-RES8 calculated from the aerobic oxidation
798 rates determined by Deshmukh et al. (2015). WD stands for warm dry (in red), WW for warm
799 wet (in grey) and CD for cool dry (in blue). The boxes show the median and the interquartile
800 range, the whiskers denote the full range of values and the plus sign (+) denotes the mean.

801
802 Figure 5: Frequency distribution of the log of CH_4 concentrations ($\mu\text{mol L}^{-1}$) at the nine
803 monitoring stations of the Nam Theun 2 Reservoir. The red, grey and blue colours indicate the
804 warm dry (WD), warm wet (WW) and cool dry (CD) seasons, respectively.

805
806 Figure 6: (a) Surface concentrations and (b) diffusive fluxes between June 2009 and
807 December 2012 at the station RES9 located at the water intake. Julian day 0 is 1st of January,
808 2009. The red, grey and blue colours indicate the warm dry (WD), warm wet (WW) and cool
809 dry (CD) seasons, respectively.

810

811 Figure 7: (a, d, g, j) stratification index (ΔT , red line, see text) and diffusive fluxes, (b,e,h,k)
812 CH_4 storage and (c,f,i,l) depth-integrated aerobic CH_4 oxidation ($\text{mmol m}^{-2} \text{d}^{-1}$, black line)
813 calculated from the aerobic oxidation rates determined by Deshmukh et al. (2015) and ΔT (red
814 line) between June 2009 and December 2012 at the stations RES1, RES3, RES7 and RES8 at
815 the Nam Theun 2 Reservoir. Julian day 0 is 1st of January, 2009. The red, grey and blue
816 colour dots indicate the warm dry (WD), warm wet (WW) and cold dry (CD) seasons,
817 respectively.

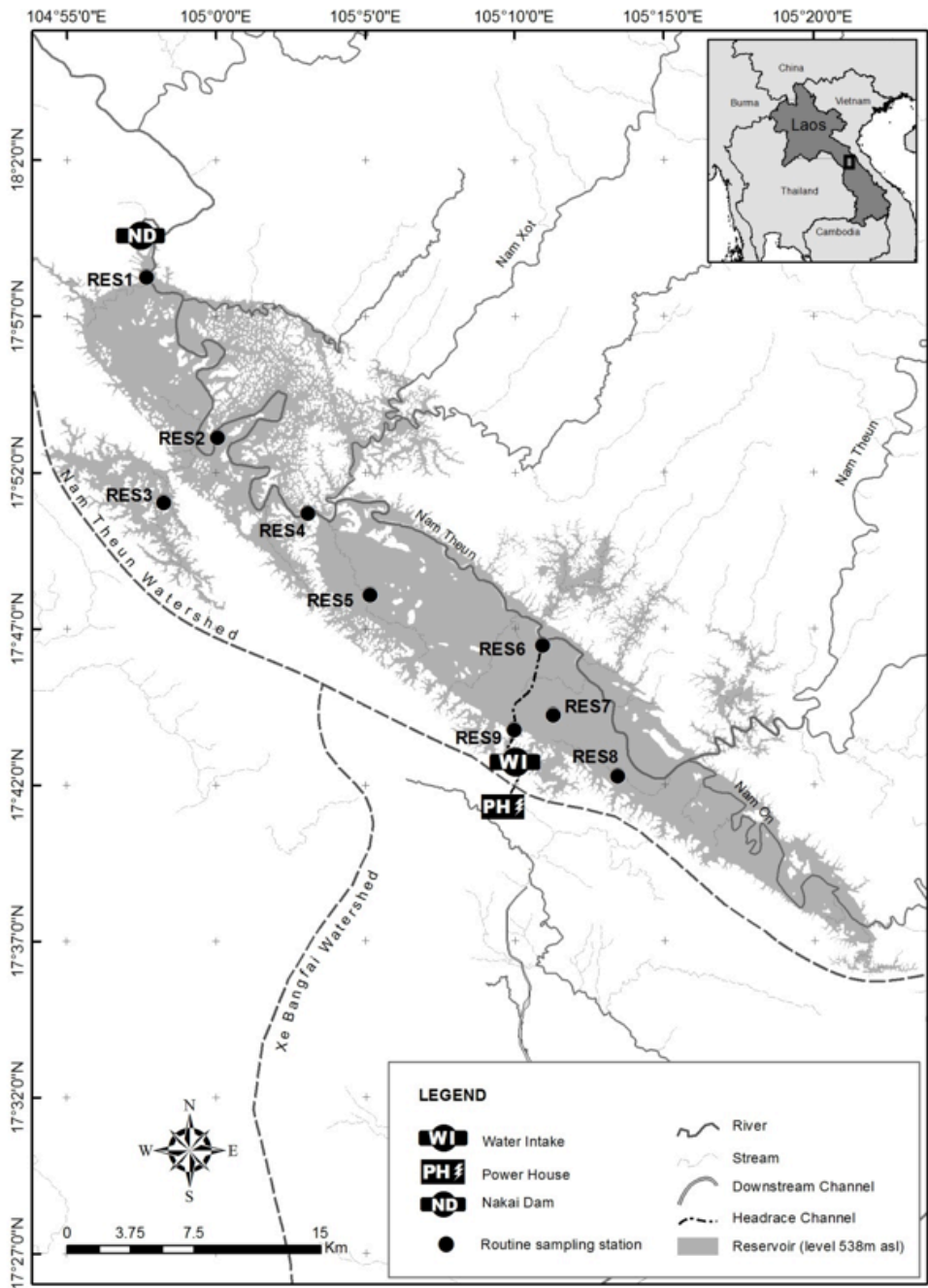
818

819 Figure 8: (a) Total emissions by diffusive fluxes in 2009, 2010, 2011 and 2012, and (b)
820 monthly emissions by diffusive fluxes between May 2009 and December 2012. Emissions
821 from RES9 (water intake) are shown in black, emissions resulting from diffusive fluxes lower
822 than $5 \text{ mmol m}^{-2} \text{d}^{-1}$ from the stations RES1 to RES8 are shown in white and emissions
823 resulting from diffusive fluxes higher than $5 \text{ mmol m}^{-2} \text{d}^{-1}$ from the stations RES1-RES8 are
824 shown in grey.

825

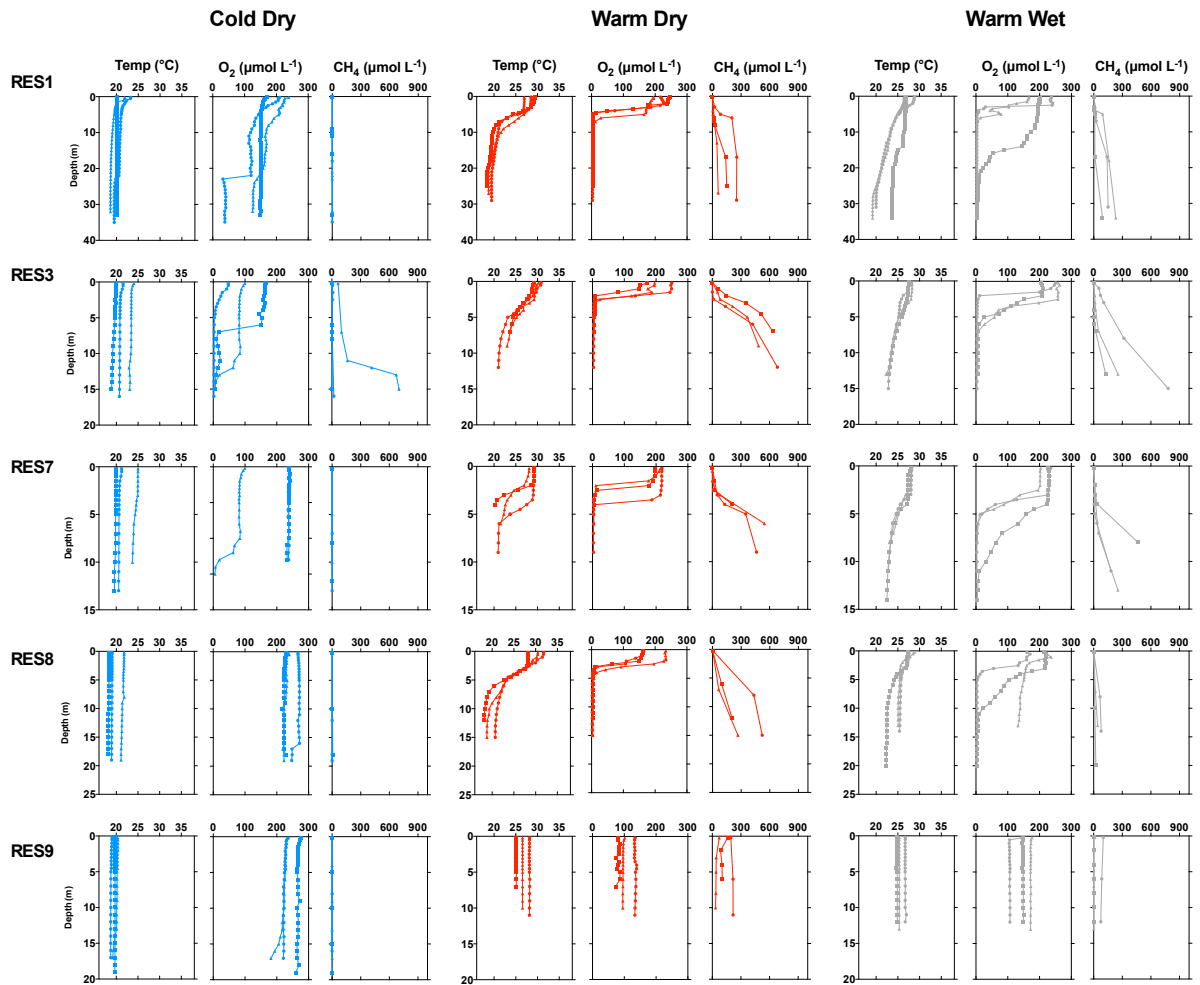
826

827
828 Figure 1
829



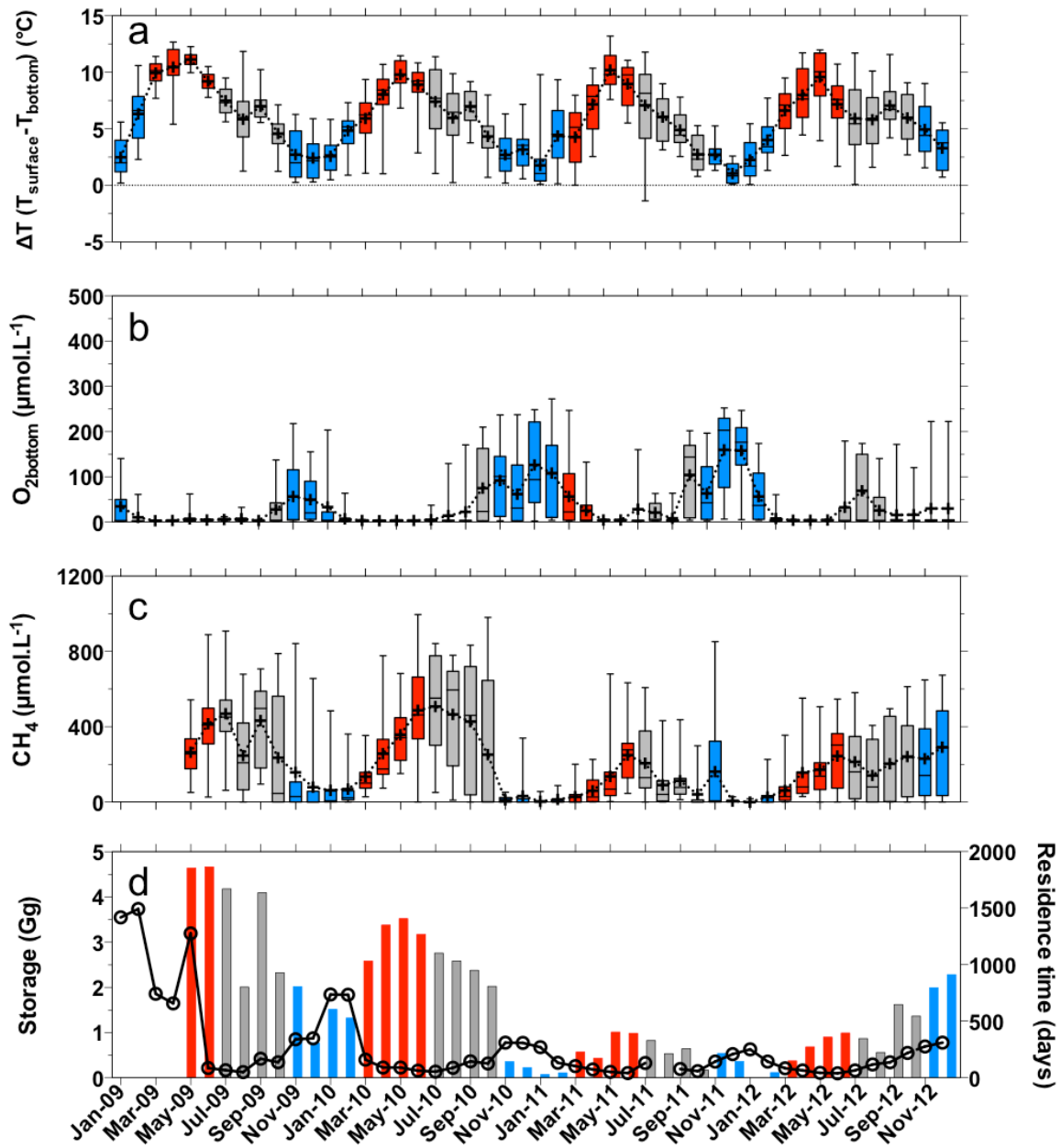
830
831
832

833
834 Figure 2
835



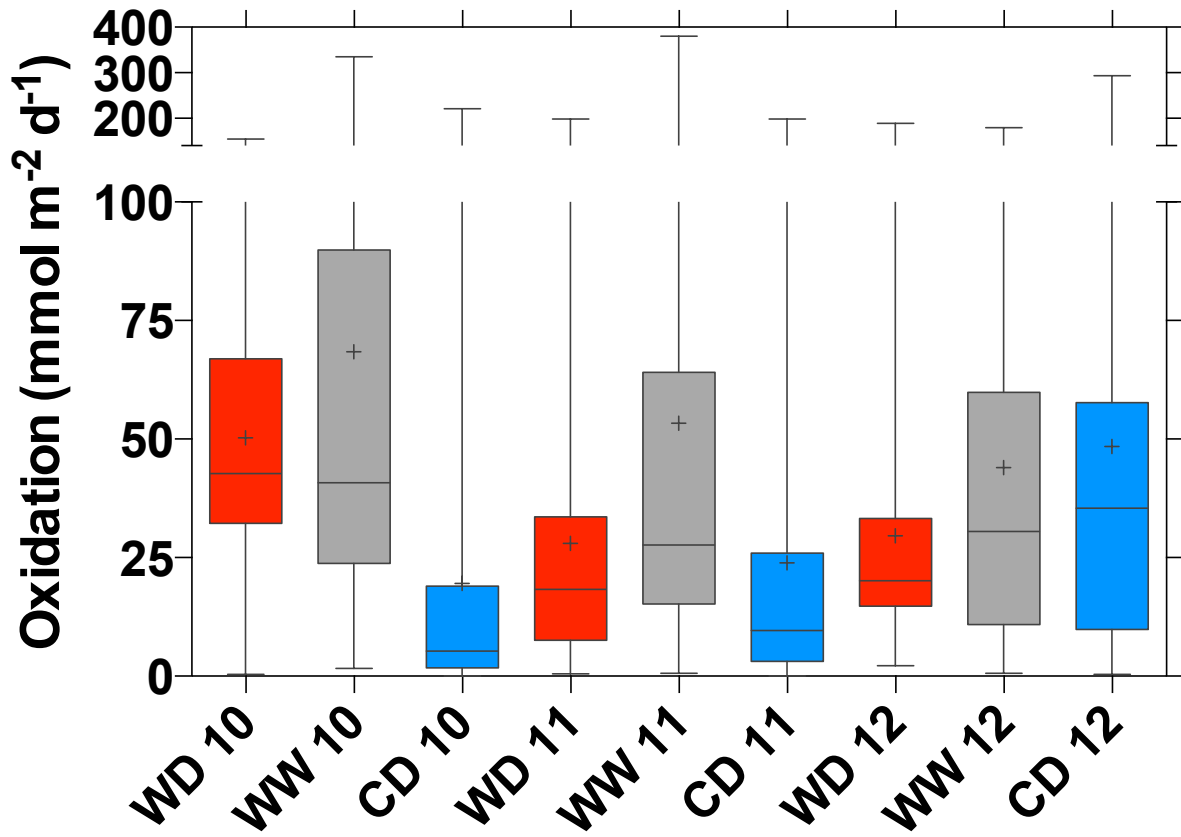
836
837
838

839
840 Figure 3
841



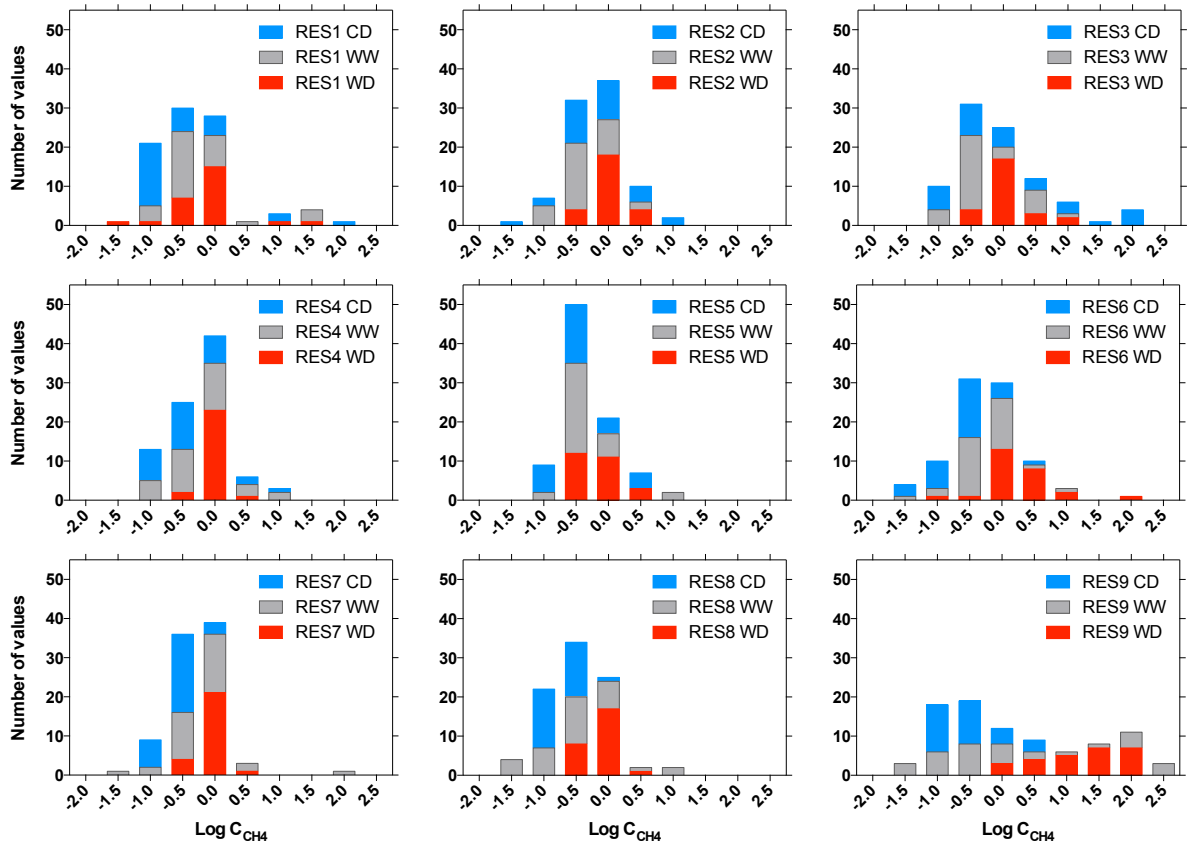
842
843
844

845
846 Figure 4
847



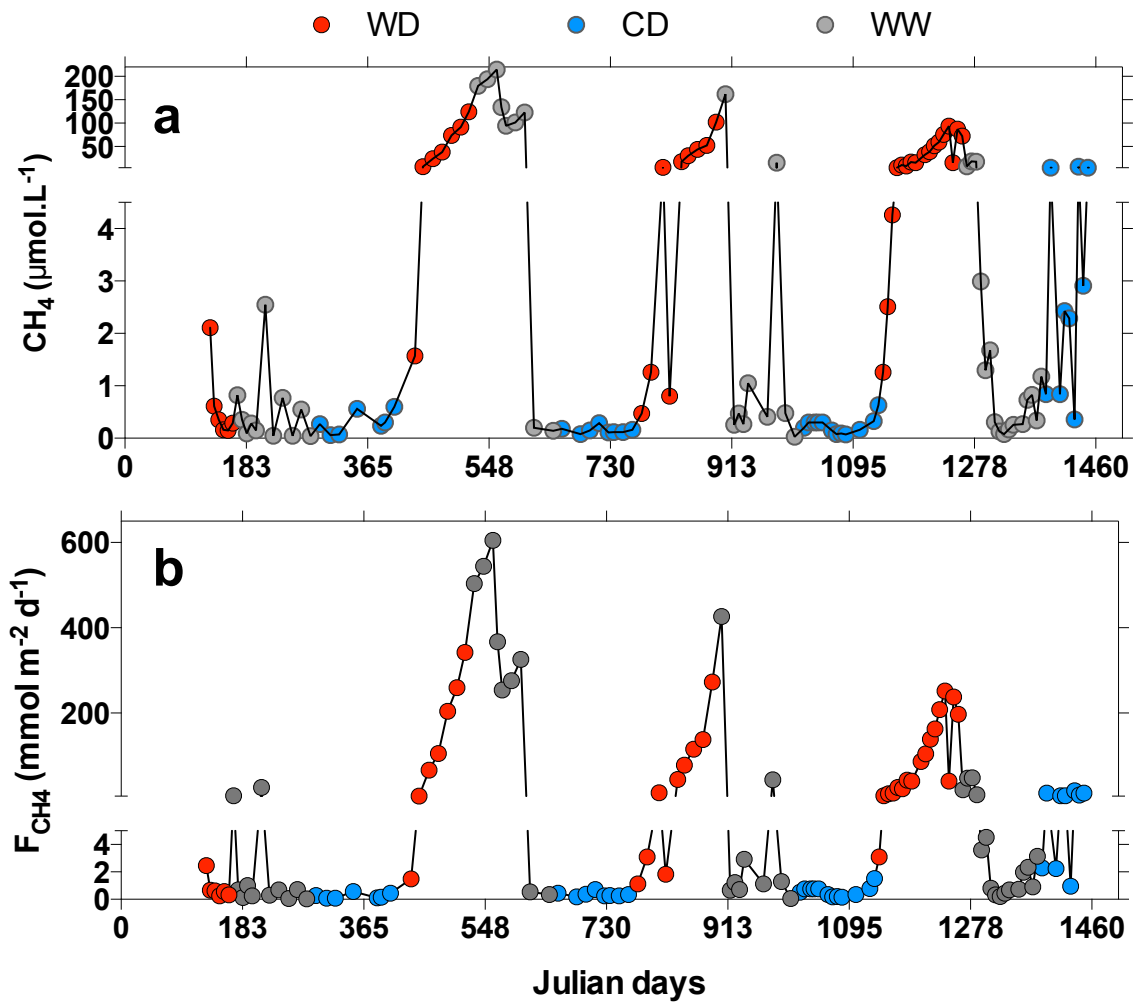
848
849
850

851
852 Figure 5
853



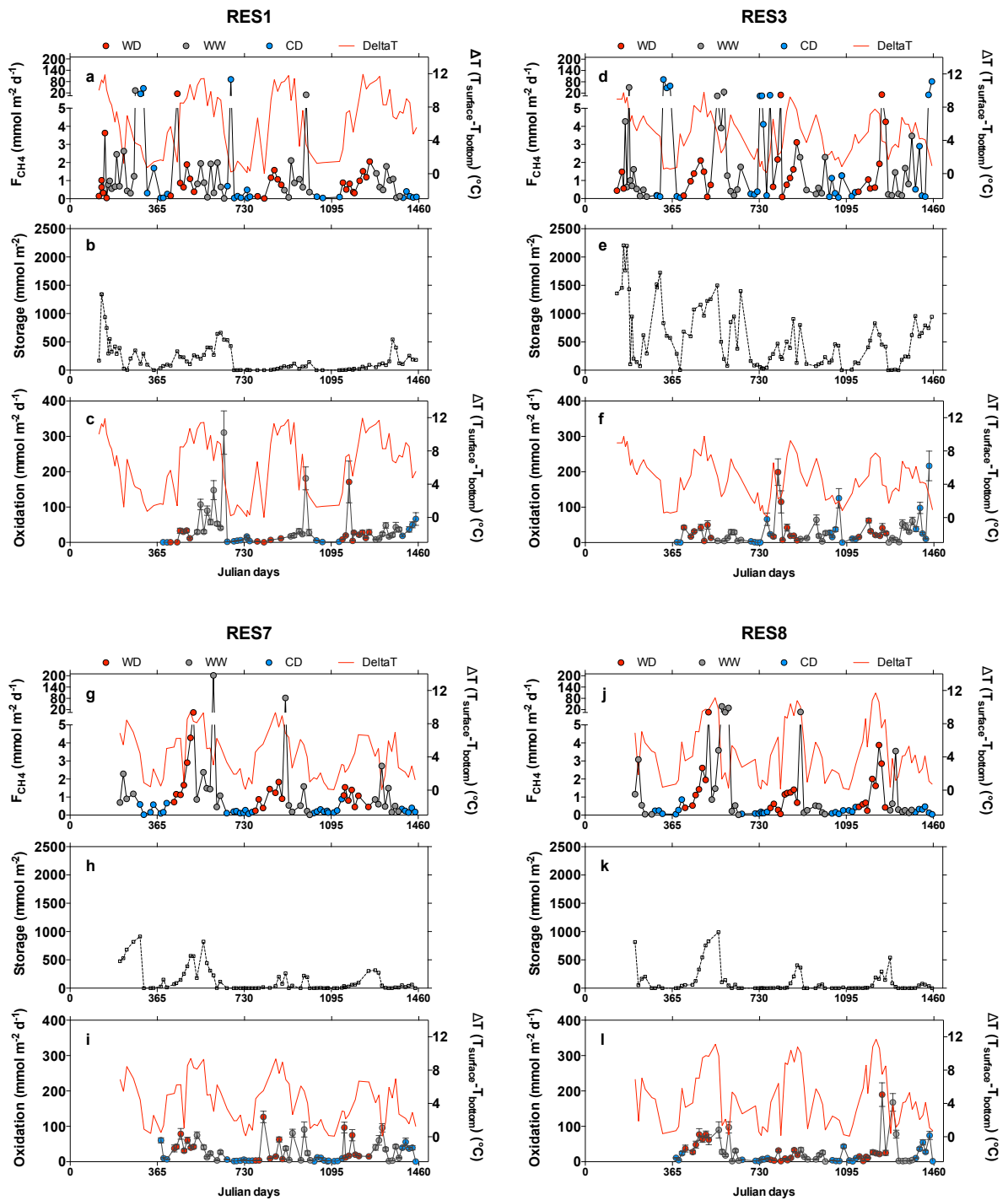
854
855
856

857
858 Figure 6
859



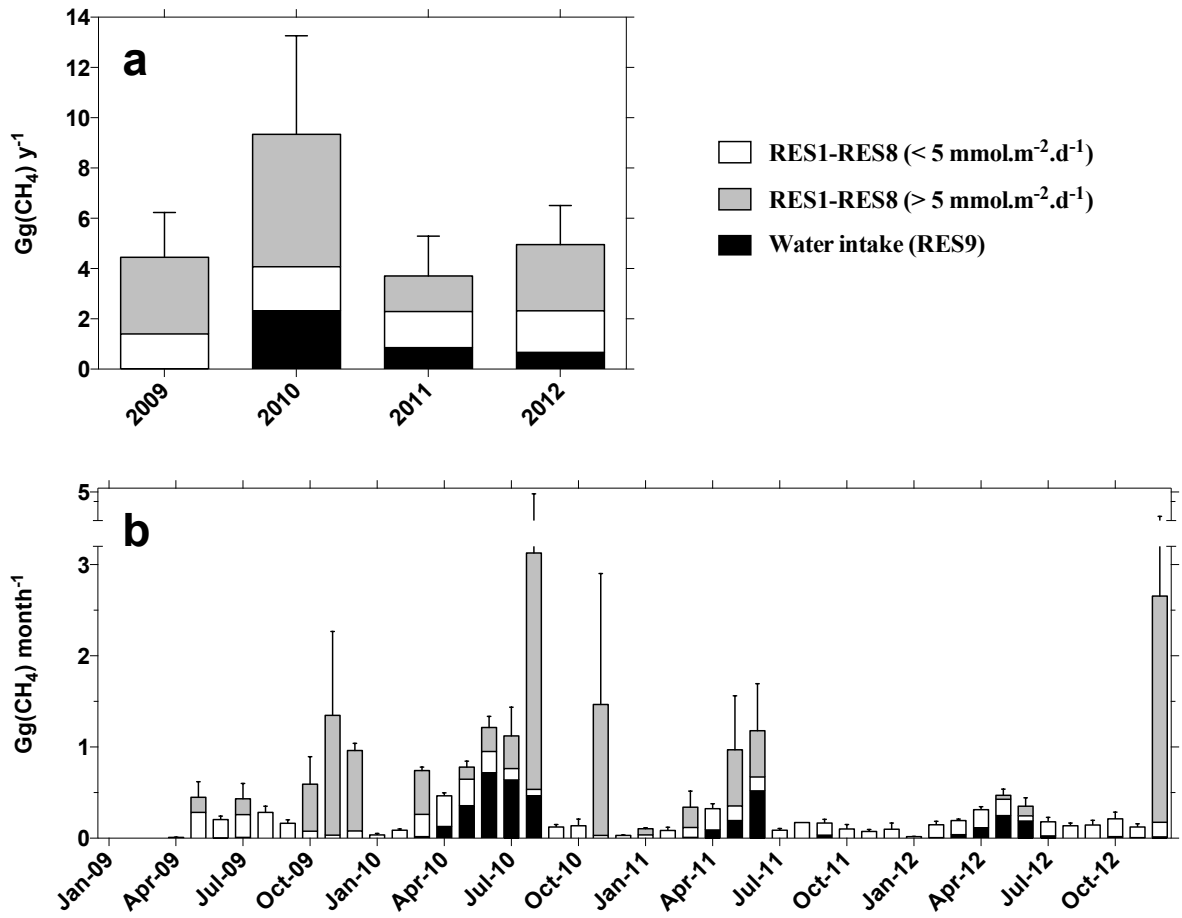
860
861
862

863
864 Figure 7
865



866
867
868

869
870 Figure 8
871



872